11TH JOINT MMM–INTERMAG CONFERENCE

January 18–22, 2010
Washington, DC

DIGESTS

HELP CONTINUE

CONFERENCE INFORMATION

www.magnetism.org

Published by the American Institute of Physics (AIP).

 ISSN 1087-3848

Reduction Design of Vibration and Noise in IPMSM type ISG for HEV

Jae-Woo Jung[1], Sang-Ho Lee[1], Geun-Ho Lee[1], Jung-Pyo Hong[1], *Senior, IEEE*,
Dong-Hoon Lee[2] and Ki-Nam Kim[3]

[1]Department of Automotive Engineering, Hanyang University, Seoul, Korea
[2]Motor R&D Center, S&T Daewoo Co., Ltd., Busan, Korea
[3]HEV System Engineering Team, Hyundai·Kia Motors, Hwaseong, Korea

Integrated starter and generator (ISG) which is one of the important components of series and parallel type hybrid electric vehicle is working as starter after vehicle idle stopping and generator during vehicle driving. When ISG works as starter to operate engine, ISG produces high torque and high power at the operating speed 4000 rpm to remove vibration of initial starting of the engine. In that time ISG produces whine noise which can be detected inside a vehicle. There are two methods to reduce the vibration and noise. One is improving the stiffness of stator and the other is reduction of electromagnetic exciting force. Although improvement of stiffness using mechanical design is utilized effectively to reduce whine noise, the electromagnetic design using the reduction of exciting forces is more reasonable in the same motor size. Because ISG produces torque ripple, radial force and tangential force on operating condition, this paper deals with the reduction design of electromagnetic exciting forces which affects the noise and vibration. Two design variables are selected to optimize the rotor shape especially geometry of flux barrier by optimization using response surface methodology (RSM). Finally, the quantity of the vibration and noise of optimized model is compared with prototype model.

***Index Terms*— IPMSM, ISG, Noise, Radial force, Tangential force, Torque ripple, Vibration**

I. Introduction

IDLE STOP is one of the most important function in hybrid electric vehicle (HEV) driving in the downtown especially. Where idle stop that ceases the engine operation in order to eliminate emission when vehicle is temporally stopped. After the idle stop, engine is started automatically by electric motor which is called integrated starter and generator (ISG) [1]. The operating speed is different between conventional engine starter and ISG which is rotating about 4000rpm with maximum power because it operates engine to reach over the idle speed to avoid a vibration of initial starting of engine. In that time, whine noise can be detected inside a vehicle. This electric noise should be removed in the electromagnetic design and optimization [2].

There are two methods to reduce the vibration and noise. One is improving the stiffness of stator and the other is reduction of electromagnetic exciting force [3]-[6]. Improvement of stiffness is utilized effectively to reduce whine noise. However, this mechanical solution brings incensement of motor size. Therefore, reduction of electromagnetic exciting force is considered in this paper. Two types of exciting force are produced during operation of ISG which are global force such as torque ripple and local force that is including radial force and tangential force [7]. This paper deals with reduction design of noise and vibration of ISG by decrease both global force and local force.

Before the improving design of ISG, we had an experiment of prototype to find source of vibration and noise. After analyzing the vibration and noise of prototype, we found that 36^{th} harmonic component of exciting force is source of vibration and noise. Therefore, reduction of 36^{th} harmonic component of exciting force is selected as an objective function of optimum design. Only two variables are selected to simplify the optimization and response surface methodology (RSM) is applied as an optimization method [8]. After design, experimental results of vibration and noise of designed model is compared with prototype to verify the design method.

Manuscript received October 31, 2009.
Corresponding author: J. P. Hong (e-mail: jphong@hanyang.ac.kr).
Digital Object Identifier inserted by IEEE

II. Noise and Vibration Characteristics of Prototype

1) Specifications of prototype

The specifications of prototype, which is designed by interior permanent magnet synchronous motor (IPMSM), are shown in Table I. Prototype is consist of 6-pole, 36-slots and wounded by distributed winding as shown in Fig. 1. Slot pitch of armature winding to get sinusoidal back electromotive force (EMF) is 5 [9]. In order to increase power density, permanent magnet of Nd-Fe-B type is inserted in the rotor. The rotor core below the permanent magnet is punched to reduce total weight of the rotor.

TABLE I
SPECIFICATIONS OF PROTOTYPE

	Values	Note
Number of pole and slots	6 / 36	-
Operating speed range	4000 rpm	Starting mode
Maximum power	6.4 kW	-
Winding method	Distributed winding	Short pitch (5/6)
Driving method	Sinusoidal wave	SV PWM

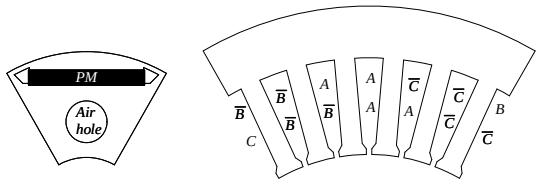

Fig. 1. Configuration of prototype

2) Experimental result of prototype

The prototype mounted beside engine is connected with shaft of engine by pulley and experimental conditions and results are shown in Fig. 2.

In order to measure vibration of prototype, 3 axis accelerometers are attached on the housing nearby cooling nipple in the radial direction and it is shown in Fig. 2 (a). In addition, noise using microphone measured 1 m away from the prototype in the direction of z-axis.

Fig. 2 (b) shows color map regarding measured vibration and noise of prototype. The vibration and noise is measured in the direction of x, y, z-axis and the trend of two results is almost similar in all direction. Because maximum torque is produced though this range of speed, the vibration and noise mainly occurred from 1600 to 3000 rpm based on prototype rotational speed. In addition, noise around 1.2 kHz after 2000 rpm in the direction of x-axis is generated by resonance of engine assembly. Source of the vibration and noise is 36th harmonic component of electromagnetic exciting force. Therefore, the source should be removed by electromagnetic design and optimization of motor shape.

Harmonic orders of electromagnetic exciting forces are shown in Table II. The fundamental component of cogging torque, 2nd harmonic component of torque ripple and 6th harmonic component of radial, tangential force are matched with 36th harmonic component of the measured vibration and noise.

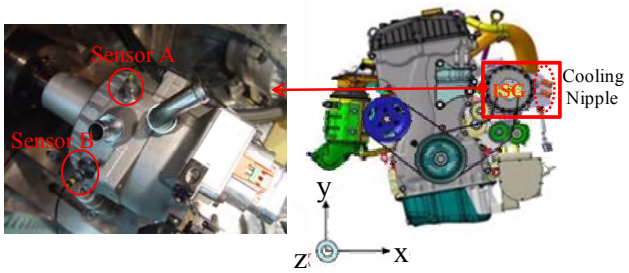

(a) Position of accelerometer

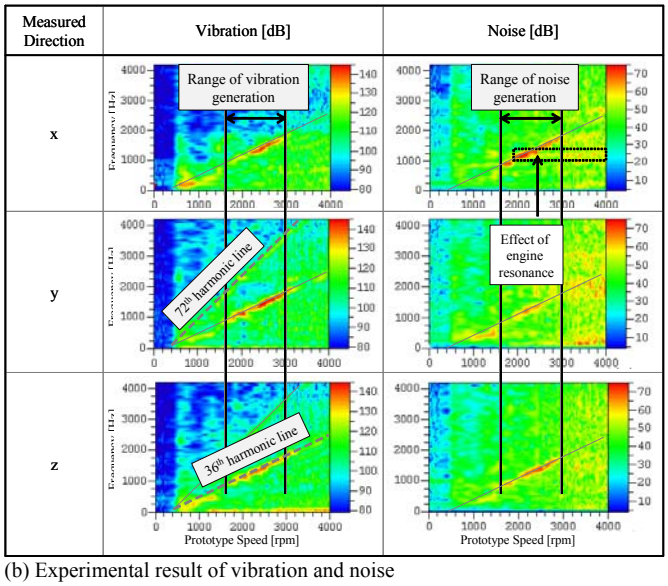

(b) Experimental result of vibration and noise

Fig. 2. Experimental result of prototype

TABLE II
HARMONIC ORDER OF ELECTORMAGNETIC EXCITING FORCES

Electromagnetic exciting forces		Harmonic order	
Global force	Cogging torque	$N/60$ X LCM_{PS} X h	$h=1,2,3,\cdots n$
	Torque ripple	$N/60$ X 6 X pp X h	
Local force	Radial force	$N/60$ X 2 X pp X h	
	Tangential force	$N/60$ X 2 X pp X h	

LCM_{PS}: Least common multiple of number of pole and slot, pp: Pole pair
N: Rotational speed of ISG, h: Harmonic order

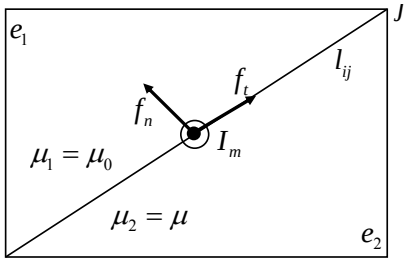

Fig. 3. Magnetizing current between the two materials

III. OPTIMIZATION OF ROTOR SHAPE

1) Calculation of local force

Fig. 3 shows the magnetizing current between the two materials. As one of the method of magnetic force calculation, magnetizing current which exists on element boundary is used equivalent magnetizing current (EMC) method and it can directly calculate the electromagnetic force which affects the surface of structure. The current I_m on the line forming element e_1 and e_2 written as (1)

$$I_m = \frac{1}{\mu_0}\int \nabla \times \vec{M} \cdot d\vec{s} = \frac{1}{\mu_0}(M_{1t} - M_{2t})l_{ij} \tag{1}$$

Where M_{1t} and M_{2t} are the tangential components of magnetization on element boundary, l_{ij} is the distance on element boundary.

$$\vec{B} = \mu_0 \vec{H} + \vec{M} \tag{2}$$

The relationship in (2) holds for all materials whether they are linear or not [10]. Substituting (2) into (1) yields.

$$I_m = \frac{1}{\mu_0}(B_{1t} - B_{2t})l_{ij} \tag{3}$$

where B_{1t} and B_{2t} are the tangential component of flux density in each material.

The electromagnetic force on the element boundary is written as

$$\vec{f}_{ij} = \vec{I}_{ij} \times \vec{B}_{ext} \tag{4}$$

Flux density value of $\vec{B}_{ext}$ is given as the average value for each element.

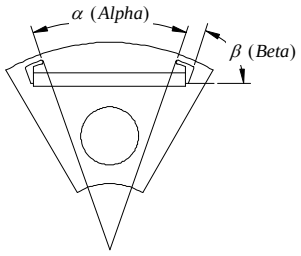

Fig. 4. Design variables for optimization

TABLE III
DESIGN AREA FOR OPTIMIZATION

Design variable	α (Alpha)	β (Beta)
Area [°]	39-42	55-64

2) Objective function and design variables

Objective function and constraint condition of optimization using RSM based on analysis of experimental results of prototype is determined as follow.

- Objective function

1. The reduction of 2nd harmonic component of torque ripple
2. The reduction of 6th harmonic component of radial and tangential force

- Constraint condition

$$T_{avg} \geq 44Nm$$

Because peak to peak value of cogging torque is relatively smaller than peak to peak value of torque wave, the fundamental component of cogging torque is excluded as the objective function.

In order to reduce time consumption for the optimization using RSM, two design variables, which are related with shape of flux barrier and pole angle, are only selected as shown in Fig. 4. Design variable α and β are related with the pole angle and shape of flux barrier and its design area are shown in Table III.

3) Result of optimization

In order to find optimal point of two design variables, the optimization using RSM is performed with using finite element analysis (FEA) [3]. From this result, the comparison of rotor shape is shown in Fig. 5. The optimal point of design variable α and β are determined by 40.5° and 65.8° , respectively as shown in Fig. 6. The shape of flux barrier which effects magnetic pole angle and leakage flux path is modified after optimization

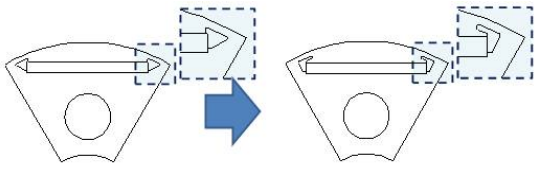

(a) Prototype (b) Optimized model

Fig. 5. The comparison of rotor shape

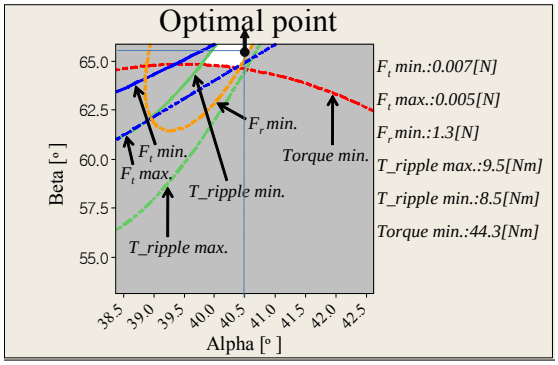

Fig. 6. Result of RSM (Optimal point)

4) Comparison of electromagnetic exciting force

Torque versus operating speed is changed to meet constant power characteristics of prototype. Therefore, radial force and tangential force are calculated with several operating speed. The 6th harmonic component of radial force and tangential force which are expected electromagnetic exciting forces of the vibration and noise are reduced as shown in Fig. 7 (a) and (b). In addition, torque ripple of the optimized model is also reduced with half value compared with prototype as Fig. 7 (c).

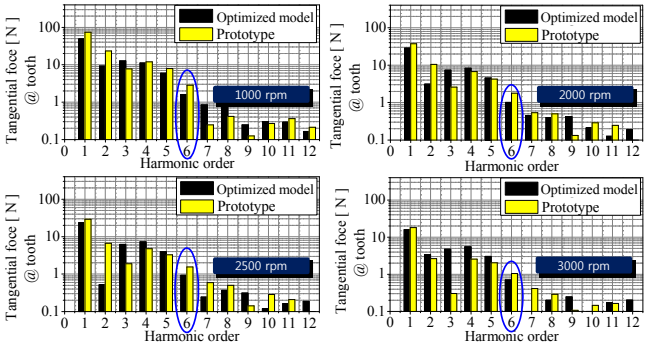

(a) Radial force

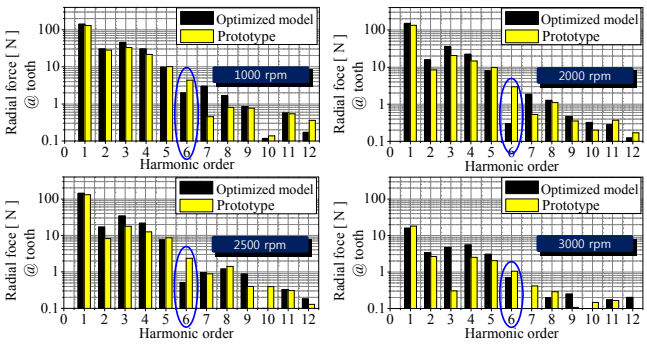

(b) Tangential force

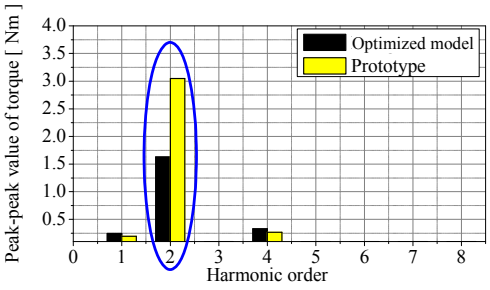

(c) Torque ripple at maximum torque

Fig. 7. Comparison of electromagnetic exciting force

IV. Experimental Result

In order to verify the validity of design method dealt with in this paper, the vibration and noise experiment is performed. Firstly, experiment based on optimized model is performed. Secondly, experiment based on vehicle is conducted to verify ultimate effect in real driving of vehicle.

Fig. 8 shows set up of experiment based on optimized model. The prototype is connected with dynamometer by pulley. Two of G sensors (accelerometer) are attached on ISG which is mentioned in Fig. 2 (a). The experiment is performed with the ISG speed 1000 rpm and 3000 rpm because the vibration and noise is maximized through 1000 rpm to 3000 rpm. In the vehicle driving, maximum torque and power are produced during 1000 rpm and 3000rpm, respectively.

Fig. 9 shows comparison of acceleration between prototype and optimized model. The vibration of optimized model is entirely lower than prototype. In addition, both total value and the 36th harmonic component of acceleration value have same trend. Accordingly, the main source of entire vibration is the 36th harmonic component.

Experiment based on vehicle is performed. The condition of experiment is that the engine of HEV is started by ISG after idle stop. Fig. 10 shows the experimental result based on vehicle experiment between designed model and prototype. Vibration and noise are also reduced in vehicle based experiment. Vibration is reduced 5 dB and noise is reduced 2 dB which is considered with A-weighting [11]. In other word, vibration and noise of optimized model is reduced half value compared with prototype.

V. Conclusion

This paper deals with the reduction design of the vibration and noise in IPMSM type ISG for HEV. Characteristics of the vibration and noise can be reduced in the magnetic circuit design by reducing electromagnetic exciting force such as radial force, tangential force and torque ripple. We analyze the experimental result of prototype and investigate the source of vibration and noise. Then optimal design is performed to minimize electromagnetic exciting forces which are 2nd harmonic of torque ripple and 6th harmonic component of radial force and tangential force. Experiment based on motor and vehicle are performed both optimized model and prototype. Optimized model is successfully reduced compared with prototype model.

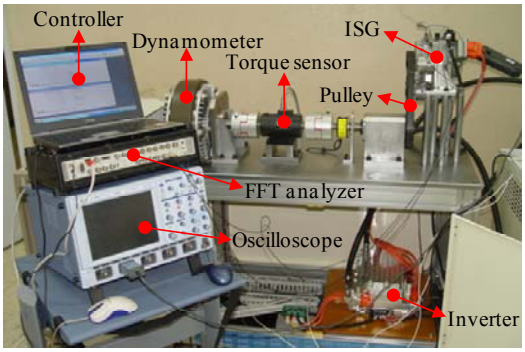

Fig. 8. Set up of experiment

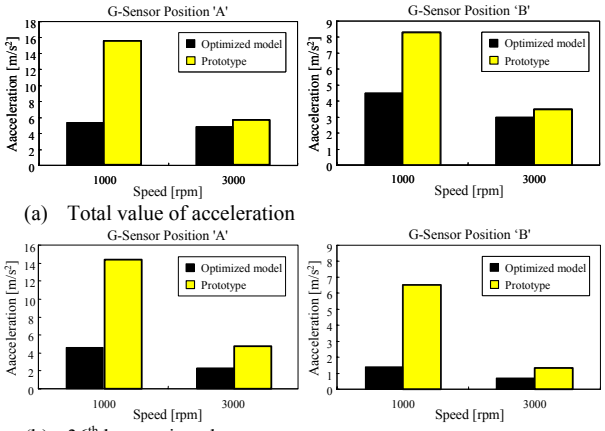

(a) Total value of acceleration

(b) 36th harmonic value

Fig. 9. Experimental result of ISG acceleration

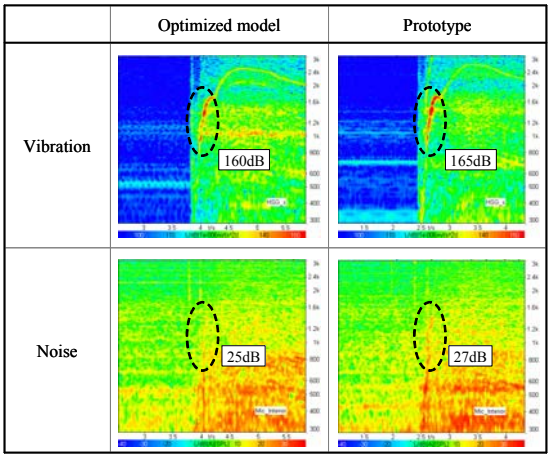

Fig. 10. Vehicle based experiment result of vibration and noise

References

[1] Friedrich, G., Girardin, A., "Integrated starter generator," *IEEE Ind. Appl. Mag.* , vol.12, no.4, pp. 26-34, July/Aug. 2009.

[2] Sung-Il Kim, Geun-Ho Lee, Jung-Pyo Hong, and Tae-Uk Jung, "Design process of interior PM synchronous motor for 43-V electric air-conditioner system in hybrid electric vehicle," *IEEE Trans. Magn.* vol. 42, no. 4, pp. 1590-1593, June 2009.

[3] Jung-Pyo Hong, Kyung-Ho Ha, and Ju Lee, "Stator pole and yoke design for vibration reduction of switched reluctance motor," *IEEE Trans. Magn.*, vol. 38, no. 2, pp.929-932, Mar. 2002.

[4] C. C. Hwang, S. P. Cheng, and C. M. Chang, "Design of High-Perforance Spindle Motors with Concentreated winding," *IEEE Trans. Magn.*, vol.41, no. 2, pp.971-973, Fbr. 2005.

[5] G. Henneberger, P. K. Sattler, and D. shen, "Nature of the equivalent magnetizing current for the force calculation," *IEEE Trans. Magn.*, vol. 28, no. 2, pp.1068-1072, Mar. 1992.

[6] Isao Hirotsuka, Yutaro Tsubouchi, and Kazo Tsuboi, "Effects of Slot Combination and Skew Slot on the Electromagnetic Vibration of a 4 pole Capacitor Motor under Load Condition," *J. Electr. Eng. Technol.*, vol. 1, no. 1, pp.85-91, Mar. 2006.

[7] G. h. Jang and D. K. Lieu, "The Effect of Magnet Geometry on Electric Motor vibration," *IEEE Trans. Magn.*, vol. 27, no. 6, pp. 5202-5204, Nov. 1991.

[8] Sung-Il Kim, Jung-Pyo Hong, Young-Kyoun Kim, Hyuk Nam, and Han-Ik Cho, "Optimal design of Slotless-Type PMLSM considering Multiple Response by Response Surface Methodology," *IEEE Trans. Magn.* vol. 42, no. 4, pp. 1219-1222, April 2006.

[9] TJE. Miller and J. R. Hendershot Jr., *Design of brushless permanent magnet motors*, Oxford Magma Physics, 1995.

[10] Matthew N. O. Sadiku, *Elements of Electromagnetics*, Oxford Univ. presss, 2001.

[11] Jacek F. Gieras, Chong Wang, and Joseph Cho Lai, *Noise of Polyphase Electric Motors*, CRC press, 2006.